Chemical Engineering Journal 115 (2006) 147–155

Chemical Engineering Journal

www.elsevier.com/locate/cej

Fragmentation on batches of coke or char particles during fluidized bed combustion

Carlos Pinho *

CEFT-DEMEGI, Faculty of Engineering, University of Oporto, Rua Dr. Roberto Frias s/n, 4200-465 Porto, Portugal

Received 31 May 2004; received in revised form 5 July 2005; accepted 6 October 2005

Abstract

During experiments being carried out on the study of batch combustion of coke or char particles in fluidized beds the evolution of the overall combustion resistance with time usually shows an apparent increase of the overall reactivity as combustion develops. This results in the reduction on the obtained value for the overall combustion resistance below what was theoretically expected.

One possible explanation for such behavior is that there is some fragmentation of the particles being thrown into the bed, leading to an increase of the external superficial area available for reaction. The augmentation of the external area increases the overall reaction rate which is erroneously interpreted as a reactivity increase of the material of the particles.

The subsequent analysis is an evaluation of the influence of particle fragmentation on the combustion rate of batches of solid particles, when such fragmentation is unknown during the analysis of the experimental data.

Keywords: Particle fragmentation; Fluidized bed combustion

1. Introduction

The fragmentation of coal or coke particles in fluidized bed combustion has been subject of discussion on the interpretation of the experimental results. Waters [1] analysing the factors that have the stronger influence upon the efficiency of fluidized bed combustion of low grade solid and liquid fuels, realized the importance of the losses of entrained carbon for high temperature conditions (enhancing thermal breakage) and high excess air conditions; these bed conditions imposed higher velocities for gaseous phase reducing the residence time of the particles in the bed disengaging height, limiting the time available for complete combustion.

In a pilot plant study on combustion of large coal particles in a fluidized bed, Gibbs and Hedley [2] stressed the relevance of particle breakage as one of the main factors affecting negatively the combustion efficiency. In their experiment, the basic idea was to reduce the importance of elutriation losses through the combustion of larger particles, but although such losses were reduced they were still higher than expected because of what the authors considered to be the relevant influence of particle fragmentation. The authors referred that the mechanism of break up of large coal particles in a hot fluidized bed had an important influence on the elutriation losses.

Peel and Santos [3] while studying essentially the fluidized bed combustion of vegetable derived fuels, have also verified combustion conditions for large size charcoal particles (2–4 and 6–10 mm) and detected that for batches of particles larger than 4 mm, there was a noisy decrepitation phenomena, i.e. thermal breakage, accompanied by fines elutriation.

Pillai [4] referred to the size alteration of coal particles through distinct modes, one of them being the break up in the case of bituminous coals. In another text [5], the same author, stressed the importance of this phenomenon, because he found out that there was particle shrinkage as burning progressed which was more often due to the progressive flaking of ash and by particle fracture, instead of consumption through normal combustion procedure.

On the paper by Ross and Davidson [6], the U-shape evolution of the overall combustion resistance with particle diameter ($1/K$ versus d), could be easily explained according to Pinho and Guedes de Carvalho [7], through the effect of particle fragmentation.

Although their paper being more on the attrition phenomenon rather than of fragmentation, Chirone et al. [8] say that frag-

* Tel.: +351 22 5081747; fax: +351 22 9537352.
E-mail address: ctp@fe.up.pt.

1385-8947/$ – see front matter © 2005 Elsevier B.V. All rights reserved.
doi:10.1016/j.cej.2005.10.001

Nomenclature

A_t	cross-sectional area of the reactor (m^2)
c_o	oxygen mole concentration at bed inlet ($kmol/m^3$)
c_p	oxygen mole concentration in the dense phase ($kmol/m^3$)
d	particle diameter (m; mm)
d_i	initial particle diameter (m; mm)
d_j	particle diameter for j size fraction (m; mm)
d_{ji}	initial particle diameter for j size fraction (m; mm)
d_s	particle diameter ignoring fragmentation (m; mm)
D_g	oxygen diffusivity in air (m^2/s)
f	burned fraction for the batch of particles (−)
f_j	burned fraction for j size fraction (−)
k'	dimensionless reaction velocity constant (−)
k_c	reaction rate constant (m/s)
k_{cs}	reaction rate constant ignoring fragmentation (m/s)
k_g	mass transfer coefficient (m/s)
K	overall reaction rate (m/s)
K_j	overall reaction rate for j size fraction (m/s)
m_c	mass of a batch of particles (kg)
n	number of size fractions (−)
N_c	number of particles in a batch (−)
N_j	number of particles for j size fraction (−)
N_{ji}	initial number of particles for j size fraction (−)
Sh	Sherwood number for a single particle $\left(\frac{k_g d}{D_g}\right)$ (−)
Sh_s	Sherwood number ignoring fragmentation (−)
t	time (s)
t_{fj}	burning time for j size fraction (s)
U	superficial velocity (m/s)

Greek letters

α_{ji}	initial diameter fraction for j size fraction (−)
ε	bed voidage fraction (−)
ϕ	parameter for the combustion model (−)
γ_{ji}	initial mass fraction for j size fraction (−)
φ	parameter for the combustion model (−)
ρ_c	particle density (kg/m^3)
σ	fragmentation ratio (−)
ψ	parameter for the combustion model (−)

mentation produces relatively coarse particles and the attrition is more important for particle losses through elutriation, thus reducing the fluidized bed combustion efficiency.

An interesting analysis is carried out by La Nauze et al. [9], on the evolution of the mass transfer coefficient as the combustion of batches of coke particles develops, and it is clearly seen from the figures shown for the evolution of the Sherwood number as a function of the particle diameter, a U-shape like trend. This trend is also shown by Pinho and Guedes de Carvalho [7], where for a given batch under analysis the evolution of the overall combustion resistance as a function of the particle diameter is that typical U-shape curve. Plotting the overall combustion resistance ($1/K$) or the Sherwood as a function of the particle diameter, for particle sizes where fragmentation is important, gives the same U-type resulting curve if the fragmentation is not accounted for. Neglecting the importance of kinetics,

$$\frac{1}{K} \propto \frac{\varphi d}{Sh D_g} \Leftrightarrow Sh \propto \frac{\varphi d}{\frac{1}{K} D_g}$$

in other words, the plot of Sh versus d is equivalent to the plot of the $1/K$ versus d. According to these last authors, for each batch this U-type evolution is typical of a combustion under the influence of the fragmentation phenomenon, which has not been accounted for in the final analysis of the experimental results.

Superimposed on the overall tendency shown in the results of La Nauze et al. [9], there is the influence, not accounted for in the data treatment, of the fragmentation leading to a misinterpretation on the number of particles composing the batch under analysis. Some comments concerning particle attrition or breakage where raised by Guedes de Carvalho and Coelho [10].

Mota et al. [11] studied the combustion of coke charges composed of a wide size distribution of particles, a situation that can be the consequence of the fragmentation of a batch of uniformly sized particles. An important conclusion of this study is that, when the combustion is controlled by the O_2 mass transfer, the fractional burn-out time is dependent upon the particle size distribution in the batch and independent of the fluidizing gas flow rate and the total mass of the batch, which means that in the event of fragmentation, although the overall mass of the charge remains the same, least the elutriation losses that can be incremented by the presence of smaller particles, there is a reaction rate increase that cannot be accounted for, if the fragmentation influence is not considered in the experimental data analysis. However, for low mass transfer resistance, a situation typical of batches composed of small particles, the fractional burn-out time is independent of the particle size distribution. It must be stressed that this situation is only important when kinetics dominate instead of diffusion and due to their smaller size, the particles are less prone to fragmentation.

Salatino and Massimilla [12] proposed a model for coal combustion where the phenomena of elutriation is taken into account, showing the concern this type of phenomena raises in modellers.

The fragmentation takes often place in the first instants after the introduction of the particles into the bed because of the thermal shock they suffer, Stubington and Moss [13], which means that a few instants after the batch feeding into the bed the number of particles effectively burning is higher than expected under no fragmentation assumption. The clarification of the importance of different reaction phenomena affecting the reaction rates is dependent upon a correct estimate of the number and size of the particles, and consequently the corresponding surface areas available for reaction [14].

More recent studies concentrate on the development of fragmentation models either through experimental methods [15] or a combination of numerical and experimental tests [16].

In the present paper, the analysis is concentrated on the observation of the influence of particle breakage upon the evaluation

of experimental data and how a U-type curve for the overall combustion resistance as a function of particle diameter easily develops as a consequence of this phenomenon.

2. Fragmentation model

A batch of carbon particles of mass m_c is composed by N_c particles of initial diameter d_i. When entering the bed, it is assumed an instantaneous breakage of all the particles composing the batch into n fractions of different sizes; for each fraction of broken particles their post-breakage initial diameter d_{ji}, is related with the pre-breakage initial diameter d_i, according to,

$$d_{ji} = \alpha_{ji} d_i \tag{1}$$

where α_{ji} is the fraction of diameter reduction for the fraction j particles ($1 < j < n$).

At the batch feeding instant the combustion has not yet started, although the particles have already broken, and the total mass of the batch of particles is the addition of the masses of the composing size fractions,

$$m_c = \sum_{j=1}^{n} m_{ji} \tag{2}$$

or

$$\rho_c \frac{\pi d_i^3}{6} N_c = \sum_j \rho_c \frac{\pi d_{ji}^3}{6} N_j \tag{3}$$

where N_j is the number of particles belonging to the size fraction j if all particle size fractions have the same particle density ρ_c equal to the initial density, while N_c is the initial number of particles.

As $d_{ji} = \alpha_{ji} d_i$, it follows that

$$\sum_j \alpha_{ji}^3 \frac{N_j}{N_c} = 1 \tag{4}$$

But as particle sizes corresponding to each fraction are different among them, the corresponding burning velocities are also different. For a given instant into the combustion process, the burned fraction f_j is dependent upon the size of the particles that were obtained through the breakage process,

$$d_j = (1 - f_j)^{1/3} \alpha_{ji} d_i \tag{5}$$

For any time during the combustion process,

$$\rho_c \frac{\pi d_s^3}{6} N_c = \sum_j \rho_c \frac{\pi d_j^3}{6} N_j \tag{6}$$

and consequently

$$\sum_j f_j \alpha_{ji}^3 \frac{N_j}{N_c} = f \tag{7}$$

where d_s is the average diameter of the particles composing the batch, in a given instant of time through the combustion and under the assumption of no fragmentation. It must also be stressed that to achieve the result shown in Eq. (7), it is assumed that the particle size ratio for each fraction resulting from the breakage stays constant during the development of the combustion process, i.e. $\alpha_{ji} = \alpha_j(t) = \text{constant}$. This is questionable as there is no experimental evidence of such occurrence, but it is adopted in the present analysis as a simplified approach.

On the other end [17] being the fluidized bed a chemical reactor, the overall reaction rate for a batch, of mass m_c, of solid particles burning inside the bed in the absence of fragmentation would be

$$\frac{1}{K} = \frac{12 d^2 m_c}{\rho_c d_i^3 A_t U k'} \tag{8}$$

where A_t is the cross-section area of the reactor, U the superficial velocity and k' is the dimensionless reaction velocity constant [17] and remembering that

$$N_c = \frac{6 m_c}{\rho_c \pi d_i^3},$$

$$\frac{1}{K} = \frac{2 d^2 N_c \pi}{A_t U k'} \tag{9}$$

In this equation, the product $N_c \pi d^2$ is the overall reaction surface comprising all the particles of the batch being burned. However, in the presence of fragmentation, the reactive area increases because there is a change in the number and size of the particles, and as such the overall reaction surface becomes $\sum_j N_j \pi \alpha_{ji}^2 (1 - f_j)^{2/3} d_i^2$, by taking into account that there are several size fractions j, composed by different numbers of particles N_j, with different diameters d_j. All these new reacting areas, corresponding to the newly formed size fractions, compete in parallel for the available oxygen, and thus the previous equation has to be modified to consider this area increase. The overall reaction resistance $1/K$ for the batch of solid particles will then be given by,

$$\frac{1}{K} = \frac{2\pi}{A_t U k'} \sum_j N_j \alpha_{ji}^2 (1 - f_j)^{2/3} d_i^2 \tag{10}$$

This last value for $1/K$ is the true value for the overall combustion resistance; however, such value is unknown in real situations, because while doing the analysis of the experimental results, the true extent of the particles fragmentation is unknown and if the influence of such fragmentation is not accounted for in the data analysis, the obtained overall combustion resistance will be,

$$\frac{1}{K_s} = \frac{2\pi}{A_t U k'} N_c d_s^2 = \frac{2\pi}{A_t U k'} N_c (1 - f)^{2/3} d_i^2 \tag{11}$$

Comparing Eqs. (10) and (11), there is a relation between the obtained value for $1/K$ in the situation of non-consideration of the particles fragmentation, i.e. the supposedly correct value $1/K_s$, and the true value for the overall resistance,

$$\frac{1}{K} = \frac{1}{K_s} \sum_j \frac{N_j}{N_c} \alpha_{ji}^2 \frac{(1 - f_j)^{2/3}}{(1 - f)^{2/3}} \tag{12}$$

Table 1
Combustion models

Combustion model	ϕ	ψ
Heterogeneous CO combustion	2	2
Homogeneous CO combustion	1	2

Considering now the theoretical definition of the overall reaction resistance $1/K$ [6,7,18] and according to the combustion model being adopted, two new equations can be obtained, respectively, one for the supposedly corrected value $1/K_s$ and other for the really correct value $1/K$,

$$\frac{1}{K_s} = \frac{\phi(1-f)^{1/3}d_i}{Sh_s D_g} + \frac{\psi}{k_{cs}} \tag{13}$$

and

$$\frac{1}{K} = \frac{\phi d}{Sh D_g} + \frac{\psi}{k_c} \tag{14}$$

where ϕ and ψ are parameters that take into account the adopted combustion model (Table 1).

Eq. (13) assumes no fragmentation, and thus for a given burned fraction of the batch f, the diameter of the particles will be a simple function of the initial diameter $d=(1-f)^{1/3}d_i$ while Sh_s and k_{cs} will be the obtained values in the assumption of no fragmentation. In the following equation, the particle diameter for a given instant along the combustion process is a more elaborate function, not only of the burned fraction and of the initial diameter, but also of the fragmentation process, being d defined as:

$$d = d_i \frac{(1-f)^{1/3}}{\left(\sum_j \frac{N_j}{N_c}\right)^{1/3}} \tag{15}$$

Consequently, d is an average equivalent diameter for the fragmented coke particles composing the batch.

Replacing Eq. (15) into Eq. (14)

$$\frac{1}{K} = \frac{\phi}{Sh D_g} \frac{(1-f)^{1/3}}{\left(\sum_j \frac{N_j}{N_c}\right)^{1/3}} d_i + \frac{\psi}{k_c} \tag{16}$$

and comparing now Eqs. (13) and (16) while taking into account Eq. (12), two equations are obtained:

$$Sh = Sh_s \frac{(1-f)^{2/3}}{\left(\sum_j \frac{N_j}{N_c}\right)^{1/3} \sum_j \left(\frac{N_j}{N_c}\alpha_{ji}^2 (1-f_j)^{2/3}\right)} \tag{17}$$

and

$$k_c = k_{cs} \frac{(1-f)^{2/3}}{\sum_j \left(\frac{N_j}{N_c}\alpha_{ji}^2 (1-f_j)^{2/3}\right)} \tag{18}$$

Eqs. (17) and (18) mean that experimental values for the Sherwood number and for the reaction rate constant k_c, obtained through combustion experiments involving particle breakage, but in presumption of absence of that phenomenon, are larger than those obtained with the full knowledge of the influence of fragmentation.

Following the analysis and assuming that there is no elutriation or disappearance of particles through consumption due to the combustion, till the moment of reaching the combustion of the fraction f, through Eqs. (17) and (18), it can be deduced that,

$$\sigma = \left[\frac{Sh_s k_c}{Sh k_{cs}}\right]^3 = \sum_j \frac{N_j}{N_c} \tag{19}$$

whereas from Eqs. (15) and (19) and as $d_s=(1-f)^{1/3}d_i$, it can be concluded that,

$$\sigma = \left(\frac{d_s}{d}\right)^3 \tag{20}$$

σ is the ratio between the total number of particles composing that batch after fragmentation and the initial number of particles, i.e. before fragmentation; it is then necessary that $\sigma > 1$ if fragmentation has taken place. This parameter is also known as the fragmentation ratio or particle multiplication factor, Zhang et al. [15]. It does not matter either the degree of fragmentation or the number of component size fractions that after fragmentation compose the bath of particles, if the corrected values for Sh and k_c for the tested situation are known, further determination of the corresponding Sh_s and k_{cs} in the ignorance of fragmentation importance of a given experiment will allow the determination whether this phenomena did or did not happen in that experiment.

When the mass fraction of each resulting fractional size is known,

$$\gamma_{ji} = \frac{m_{ji}}{m_c} \tag{21}$$

and then,

$$\frac{\pi d_{ji}^3}{6}\rho_c N_j = \gamma_{ji}\frac{\pi d_i^3}{6}\rho_c N_c \tag{22}$$

which gives

$$\frac{N_j}{N_c} = \frac{\gamma_{ji}}{\alpha_{ji}^3} \tag{23}$$

From Eqs. (4) and (5) and taking into account that $\sum_j \gamma_{ji} = 1$,

$$\sum_j \gamma_{ji} f_{ji} = f \tag{24}$$

Eq. (12) will then be written as

$$\frac{1}{K} = \frac{1}{K_s}\sum_j \left[\frac{\gamma_{ji}}{\alpha_{ji}}\frac{(1-f_j)^{2/3}}{(1-f)^{2/3}}\right] \tag{25}$$

as well as Eqs. (15), (17) and (18)

$$d = d_{\mathrm{i}} \frac{(1-f)^{1/3}}{\left(\sum_j \frac{\gamma_{ji}}{\alpha_{ji}^3}\right)^{1/3}} \tag{26}$$

$$\frac{Sh}{Sh_{\mathrm{s}}} = \frac{(1-f)^{2/3}}{\left(\sum_j \frac{\gamma_{ji}}{\alpha_{ji}^3}\right)^{1/3} \sum \frac{\gamma_{ji}}{\alpha_{ji}} (1-f_j)^{2/3}} \tag{27}$$

$$\frac{k_{\mathrm{c}}}{k_{\mathrm{cs}}} = \frac{(1-f)^{2/3}}{\sum_j \frac{\gamma_{ji}}{\alpha_{ji}} (1-f_j)^{2/3}} \tag{28}$$

and also Eq. (19) becomes now

$$\sigma = \sum \frac{\gamma_{ji}}{\alpha_{ji}^3} \tag{29}$$

These previous equations allow the comprehension of the influence of particle breakage upon the kinetic results obtained in laboratory experiments; how the Sherwood and reaction rate constant values become masked by the influence of this phenomenon.

To simulate the experimental results that are obtained from a set of laboratory experiments, it is still necessary to relate the burned fractions corresponding to any two fractional particle sizes. To achieve this purpose, it is necessary to consider the combustion rate of a single coke particle. From the mass rate of carbon consumption through combustion of a single particle, it can be written that [6,7,18],

$$-\frac{1}{K_j} \mathrm{d}d_j = \frac{48 c_{\mathrm{p}}}{\rho_{\mathrm{c}}} \mathrm{d}t \tag{30}$$

where c_{p} is the mole concentration of oxygen inside the bed and replacing the overall c_{p} combustion resistance according to its definition, Eq. (14),

$$-\mathrm{d}d_j \left(\frac{\phi d_j}{Sh D_{\mathrm{g}}} + \frac{\psi}{k_{\mathrm{c}}} \right) = \frac{48 c_{\mathrm{p}}}{\rho_{\mathrm{c}}} \mathrm{d}t \tag{31}$$

Considering that ϕ and ψ are independent from the particle size, which seems to be a correct assumption for particle combustion in bubbling fluidized beds as some recent experiments confirm homogeneous CO reactions [11,19] for particles above 1 mm, situation where fragmentation has some importance, this last equation can be easily integrated giving

$$\frac{\phi(d_{ji}^2 - d_j^2)}{2 Sh D_{\mathrm{g}}} + \frac{\psi(d_{ji} - d_j)}{k_{\mathrm{c}}} = \frac{48}{\rho_{\mathrm{c}}} \int_0^{t_{\mathrm{f}j}} c_{\mathrm{p}} \, \mathrm{d}t \tag{32}$$

The second member of the above equation is independent from the particle size fraction under analysis, be it a particle from size fraction d_j or from d_k because it is only a function of the reactor type through c_{p}, the oxygen mole concentration. The time elapsed is the same as all fractions resulting from breakage burn simultaneously, although the corresponding burned fraction will be different; as $d_j = (1-f_j)^{1/3} d_{ji} = (1-f_j)^{1.3} \alpha_{ji} d_{\mathrm{i}}$, a relation between the burned fraction of two fractions of particles having different sizes and created through the fragmentation process is then obtained,

$$\frac{\phi[1-(1-f_j)^{2/3}]\alpha_{ji}^2 d_{\mathrm{i}}}{2 Sh D_{\mathrm{g}}} + \frac{\psi[1-(1-f_j)^{1/3}]\alpha_{ji}}{k_{\mathrm{c}}} = \frac{\phi[1-(1-f_k)^{2/3}]\alpha_{ki}^2 d_{\mathrm{i}}}{2 Sh D_{\mathrm{g}}} + \frac{\psi[1-(1-f_k)^{1/3}]\alpha_{ki}}{k_{\mathrm{c}}} \tag{33}$$

By means of the system of Eqs. (23), (27)–(29) and (33) and that $\sum_j \gamma_{ji} = 1$, it is possible to plot the evolution of Sh/Sh_{s}, $k_{\mathrm{c}}/k_{\mathrm{cs}}$ and σ for a batch of coke particles whose fragmentation is known.

3. Influence of fragmentation on the physical and kinetic parameters

As referred in the previous section through the plot of some characteristic situations the impact of the fragmentation on the experimental results obtained through the analysis of a given experiment can be assessed through an example like that considered in Fig. 1.

In the graph of this figure, the evolution of a proposed practical situation can be evaluated. The graph was built for the following conditions. It was supposed that for a given batch, 50% (w/w) of the particles kept their initial diameter while the other half underwent fragmentation as soon as they were thrown into the bed at 900 °C. In terms of the several characterizing parameters it means that $\alpha_{1i} = 1$, $\gamma_{1i} = \gamma_{1i} = 50\%$, and the overall burned mass fraction considered took three values, $f = 0$, 25 and 50%, respectively. Initial particle size was assumed to be 1 mm, $\phi = 1$, $\psi = 2$ and $Sh = 1 \approx 2\varepsilon$.

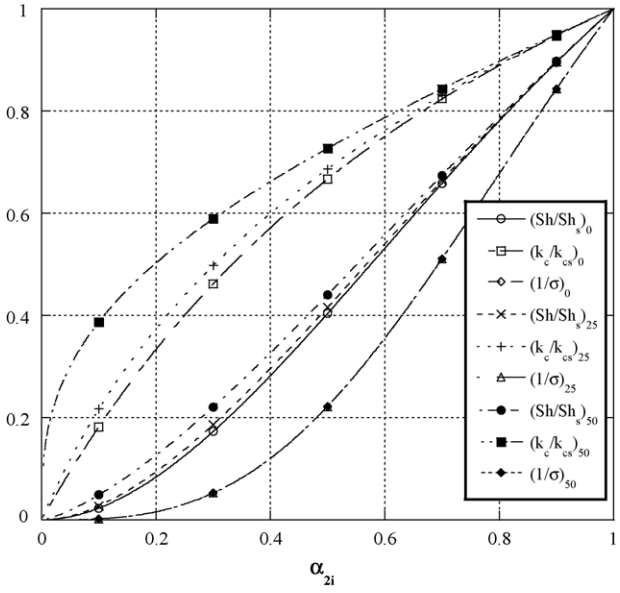

Fig. 1. Evolution of physical and kinetic parameters with particle fragmentation for three mass burned fractions, 0, 25 and 50% as indicated by the corresponding subscripts on the legend.

Curves identified with the subscript 0 refer to the initial instant subsequently to the fragmentation occurring immediately after batch introduction inside the bed, when $f = f_1 = f_2 = 0$, situation where Eq. (33) was not required for the calculations. Plotted curves result from the immediate application of Eqs. (27)–(29). As combustion evolves, for $f = 25$ and 50%, Eq. (33) is now required to obtain f_1 and f_2, according to the amount of fragmentation suffered by the fragile half-batch, characterized through the parameter α_{2i}. The inverse of the fragmentation ratio $1/\sigma$ changes according to the extension of fragmentation, but is of course the same for any burned mass fraction. In every situation, $1/\sigma < 1$which means that through the breakage there is an increase on the number of particles constituting the batch undergoing combustion.

As far as the ratio Sh/Sh_s is concerned, its value is the lowest at the beginning of the combustion, suffering an attenuation with the progression of the reaction as can be seen by the relative position of the curves for 25 and 50% of burnout mass fraction. For every circumstances, the conclusion is that the real value of the Sherwood number is lower than the obtained value in the supposition of non-breakage conditions.

For the kinetic data, the evolution is the opposite, as combustion develops the discrepancies between the real and the assumed value increase, although once again the real value is lower than the value obtained in the supposition of non-breakage conditions.

A general conclusion that can be drawn from Fig. 1 is that the fragmentation phenomena leads to an underestimation of mass transfer and of kinetic data.

4. Batch combustion with different degrees of fragmentation

To get a better understanding of the implication of the impact of fragmentation on the experimental results, a simulation of the combustion of a batch of carbon particles can be easily achieved as explained. It is assumed that a batch of 2.8 g of coke particles, with an initial size of 1.08 mm, is introduced into a bed at 900 °C; carbon burns to CO at the surface of the particles, $\phi = 1$, $\psi = 2$, and it is considered that $Sh = 1 \approx 2\varepsilon$ [7]. The coke particles suffer initial breakage into several size fractions with different sizes. Five situations were accounted for, as seen in Table 2.

To simulate the combustion of a batch of particles suffering immediate fragmentation after being introduced into the fluidized bed, the calculation process is as follows. The overall combustion resistance of the size fraction j is calculated through the adaptation of Eq. (14), to this particular size under consideration,

$$\frac{1}{K_j} = \frac{\phi d_j}{Sh D_g} + \frac{\psi}{k_c} \tag{34}$$

assuming that for each size fraction j there is no further particle breakage. From Eq. (9), it is obtained that

$$k'_j = \frac{2\pi d_j^2 N_j K_j}{A_t U} \tag{35}$$

Table 2
Fragmentation cases

Case	Size fractions		
1	1	$N_1 = 3121$	$\gamma_{1i} = 1$
2	1	$N_1 = 6325$	$\gamma_{1i} = 1$
		$N_2 = 0$	$\gamma_{2i} = 0$
3	3	$N_1 = 1873$	$\gamma_{1i} = 0.60$
		$N_2 = 1524$	$\gamma_{2i} = 0.25$
		$N_3 = 3745$	$\gamma_{3i} = 0.15$
4	4 (at 0 s)	$N_1 = 1561$	$\gamma_{1i} = 0.5$
		$N_2 = 1849$	$\gamma_{2i} = 0.25$
		$N_3 = 3121$	$\gamma_{3i} = 0.125$
		$N_4 = 24968$	$\gamma_{4i} = 0.125$
5 (sequential fragmentation)	4 (at 0 s)	$N_1 = 3121$	$\gamma_{1i} = 1$
		$N_2 = 0$	$\gamma_{2i} = 0$
		$N_3 = 0$	$\gamma_{3i} = 0$
		$N_4 = 0$	$\gamma_{4i} = 0$
	4 (at 5 s)	$N_1 = 1873$	$\gamma_{1i} = 0.6$
		$N_2 = 1524$	$\gamma_{2i} = 0.25$
		$N_3 = 3745$	$\gamma_{3i} = 0.15$
		$N_4 = 0$	$\gamma_{4i} = 0$
	4 (at 10 s)	$N_1 = 562$	$\gamma_{1i} = 0.3$
		$N_2 = 1365$	$\gamma_{2i} = 0.25$
		$N_3 = 12191$	$\gamma_{3i} = 0.25$
		$N_4 = 184948$	$\gamma_{4i} = 0.2$

where N_j is the number of particles in that size fraction, whereas the k' for the batch is given by,

$$k' = \frac{2\pi}{A_t U} \sum_j d_j^2 N_j K_j \tag{36}$$

After k' is obtained, the average oxygen concentration inside the bed, as the combustion develops, can be determined through [18],

$$c_p = \frac{c_o}{k' + 1} \tag{37}$$

with c_o as the oxygen mole concentration at the entrance of the bed. The knowledge of the oxygen concentration inside the reactor is fundamental for the calculation of the size evolution of the particles being burned, through Eq. (39) ahead.

Again from Eq. (11), the supposedly correct overall combustion resistance for the batch is determined,

$$\frac{1}{K_s} = \frac{2 d_s^2 N_c \pi}{A_t U k'} \tag{38}$$

where N_c is the total number of particles composing the batch before fragmentation (and in the ignorance of this event), and d_s is the average particle diameter ignoring fragmentation and on the first calculation step $d_s = d_i$.

The next step is the calculation of the reduction of the diameter of the particles as they burn, and this for every size fraction being considered. According to Eq. (30), it can be written that

$$\frac{d}{dt}(d_j) = -\frac{48 K_j c_p}{\rho_c} \tag{39}$$

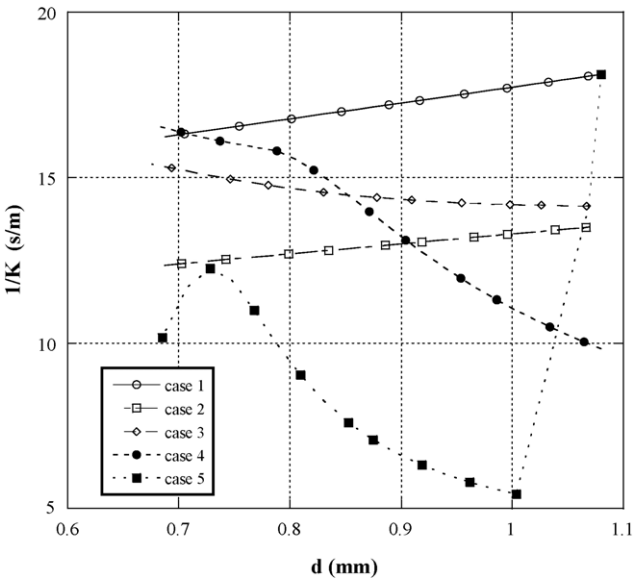

Fig. 2. Evolution of the overall resistance for the combustion of a batch of char particles. Batch size of 2.8 g, of particles with an initial diameter of 1.08 mm, burning in a fluidized bed at 900 °C. Five different fragmentation situations were considered, as referred in Table 2.

with K given by Eq. (34) and c_p by Eq. (37). A finite reduction on diameter Δd_j is then calculated as a function of a given time increment Δt, such that $d_j = (d_j)_{old} + \Delta d_j$, and afterwards,

$$d_s = \left(\sum_j d_j^3 \frac{N_j}{N_c} \right)^{1/3} \quad (40)$$

The calculation procedure restarts from Eq. (34) along another calculation step until the historic of the batch combustion is obtained.

In Fig. 2, case 1 refers to the combustion of the batch in the absence of particle breakage. Overall combustion resistance is the greatest found. When there is initial breakage and a single size fraction is formed, case 2, and this phenomenon is not taken into consideration, it is evident from the corresponding $1/K$ versus d plot that erroneous information concerning mass transfer and kinetic data are obtained from the slope and intercept of the line. This leads to the conclusion that $Sh > 1$ and that $k_{cs} > 0.15$ m/s. This last result would lead to the conclusion that the temperature of the particles would be above bed temperature, which is not the case. Case 3 considers another situation of initial particle fragmentation, now two extra size fractions are obtained and the result is a slightly negative slope and in the final part the curve would approach that corresponding to a non-breakage situation. As fragmentation gets stronger, case 4, the evolution of the overall resistance of combustion shows a sudden initial drop in the obtained value. This curve is typical of strong fragmentation in the beginning of the combustion process as shown in the experimental results of plotted in Fig. 1 of Pinho and Guedes de Carvalho [7].

Case 5 is the result of a sequential fragmentation. In such circumstances, there is not only the initial breakage after the introduction of the batch into the bed, but particles keep on breaking, and consequently their number as well as the total surface area available for reaction increase continuously. If these events are not taken into account, for the experimental data interpretation, the resulting $1/K$ versus d plot, gives a U-type like curve, as obtained from the laboratory experiments.

5. Comparison with experimental data

The results of two experiments obtained with two batches of 2.9 g, of particles with a nominal diameter of 3.1 m, and for two different cokes (Table 3) are now analysed under the light of the present model. The nominal diameter is the arithmetic mean of the mesh sizes for two consecutive sieves and in Table 3, the corresponding effective diameters are presented. These experiments were carried out in a laboratory scale fluidized bed reactor, as described by Pinho and Guedes de Carvalho [7], at a bed temperature of 900 °C.

Coke A (Table 3), is fragile and particle breakage is easily audible and occurs immediately after their introduction into the fluidized bed reactor. In such circumstances, the effective number of particles greatly increases but as the operator is not

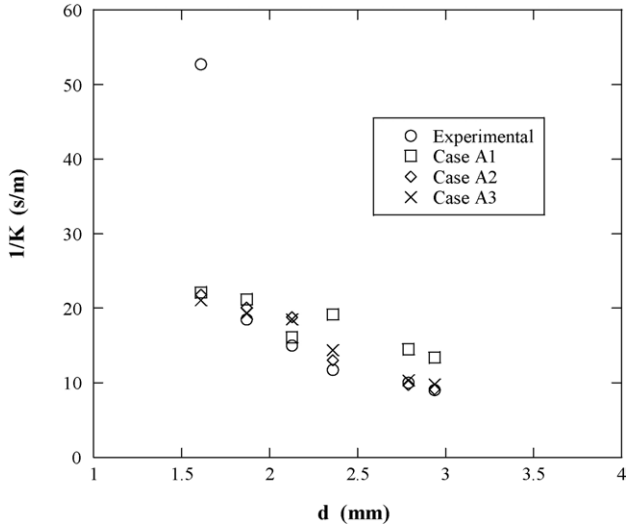

Fig. 3. Overall combustion resistance for coke A particles. Batch size 2.9 g of 3.1 mm particles; bed temperature 900 °C; superficial velocity 300 mm/s.

Table 3
Characteristics of the tested cork batches

Coke type	d_i (mm)	Specific gravity (−)	Carbon (%)	Volatile matter (%)	Moisture (%)	Ashes (%)	ρ_c (kg/m^3)	N_c (−)
A	3.01	1.705	80.02	5.51	Traces	12.47	1364	150
B	3.08	1.740	83.62	3.49	Traces	11.89	1455	130

Nominal diameter of particles 3.1 mm and batches of 2.9 g.

Table 4
Coke A, simulated fragmentation in a batch of 150 particles

Case	Size fractions		
A1	4 (at 0 s)	$N_1 = 75$	$\gamma_{1i} = 0.5$
		$N_2 = 110$	$\gamma_{2i} = 0.25$
		$N_3 = 150$	$\gamma_{3i} = 0.125$
		$N_4 = 1202$	$\gamma_{4i} = 0.125$
A2	4 (at 0 s)	$N_1 = 45$	$\gamma_{1i} = 0.3$
		$N_2 = 110$	$\gamma_{2i} = 0.3$
		$N_3 = 120$	$\gamma_{3i} = 0.1$
		$N_4 = 2825$	$\gamma_{4i} = 0.3$
A3	4 (at 0 s)	$N_1 = 45$	$\gamma_{1i} = 0.3$
		$N_2 = 110$	$\gamma_{2i} = 0.3$
		$N_3 = 180$	$\gamma_{3i} = 0.15$
		$N_4 = 2405$	$\gamma_{4i} = 0.25$

aware of such situation, the interpretation of the experimental data leads to a strong reduction on the overall resistance of the combustion reaction during the first instants, and the resulting plot of experimental data for $1/K$ versus d has a negative slope, in opposition to what is theoretically correct, white circles in Fig. 3. To interpret such trend, the proposed model was applied to this situation by assuming three different breakage levels, with four different size fractions, as detailed in Table 4, all occurring at instant 0 s. The corresponding calculated points for the combustion simulation are also presented in the same Fig. 3. The proposed breakage levels are similar in terms of the size reduction taking place, only the mass fraction of the size fractions differ. With the exception of case A1, simulation results closely follow the experimental points. At the end of the combustion, for particle diameters around 1.6 mm, which is equivalent to a mass burned fraction of 85%, further breakage not accounted in the considered single step breakage situations, explains the discrepancies among experimental results of 52.7 m/s and the numerical results around 21 m/s. This was intentional, to show how even a crude approach to the breakage process could result in an acceptable fitting between experimental and numerical results.

Coke B (Table 4) is more robust and the crepitation was not so evident, meaning that particle breakage was not so violent. The fragmentation took place in a smoother way along the combustion of the particles, as is understandable from the analysis of the U-type evolution of $1/K$ versus d, again for a batch of 2.9 g of 3.1 mm particles of nominal size (Fig. 4). The experiment was also carried out at 900 °C, but the superficial velocity was of 500 mm/s.

Table 5
Coke B, simulated fragmentation in a batch of 130 particles

Case	Size fractions		
B1 (sequential fragmentation)	4 (at 0 s)	$N_1 = 130$	$\gamma_{1i} = 1$
		$N_2 = 0$	$\gamma_{2i} = 0$
		$N_3 = 0$	$\gamma_{3i} = 0$
		$N_4 = 0$	$\gamma_{4i} = 0$
	4 (at 30 s)	$N_1 = 78$	$\gamma_{1i} = 0.6$
		$N_2 = 54$	$\gamma_{2i} = 0.3$
		$N_3 = 38$	$\gamma_{3i} = 0.1$
		$N_4 = 0$	$\gamma_{4i} = 0$
	4 (at 250 s)	$N_1 = 23$	$\gamma_{1i} = 0.3$
		$N_2 = 38$	$\gamma_{2i} = 0.3$
		$N_3 = 114$	$\gamma_{3i} = 0.3$
		$N_4 = 104$	$\gamma_{4i} = 0.1$

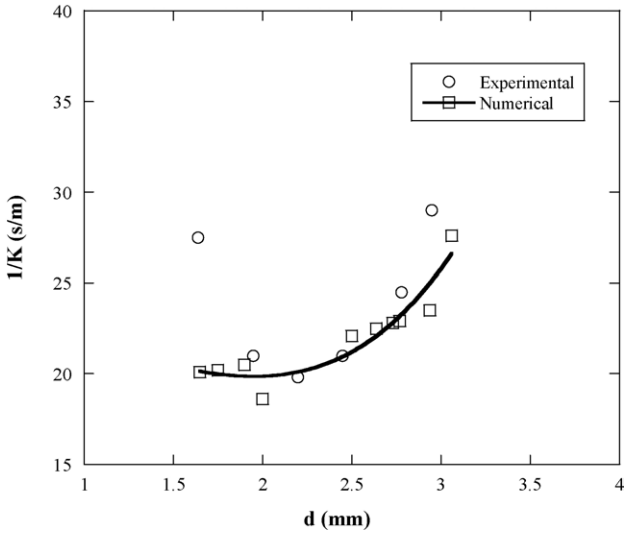

Fig. 4. Overall combustion resistance for coke B particles. Batch size 2.9 g of 3.1 mm particles; bed temperature 900 °C; bed superficial velocity 500 mm/s. The continuous line is a third-order polynomial fitting to the numerical points, for the fragmentation case shown in Table 5.

To evaluate the influence of particle fragmentation on the evolution of the overall combustion resistance of this coke B, a breakage model composed by three fragmentation steps into four sizes was adopted (Table 5). Instead of going towards a larger number of fragmentation steps, guaranteeing the closest fitting of the numerical results to the experimental results, a simpler fragmentation sequence was chosen. As a result of this, at the end of the combustion of the batch, discrepancies among experimental and numerical points increase once more (Fig. 4), but again the combustion has reached around 85% completion and experimental data beyond this limit are not very much reliable. However, the overall trend of the evolution of $1/K$ versus d is clearly followed by the results of the numerical simulation, as shown by the continuous line, which is a third-order polynomial fitting to the numerical points.

The simulations concerning cokes A and B were again calculated for carbon combustion to CO at the surface of the particles, i.e. $\phi = 1$ and $\psi = 2$, and for $Sh = 1 \approx 2\varepsilon$ [7].

6. Conclusions

The fragmentation of batches of carbon particles in laboratory scale fluidized beds, if not properly accounted for, can lead to erroneous interpretation of the experimental results.

A model was presented to show that, if the fragmentation phenomenon was ignored, physical and kinetic results can be underestimated.

If corrected physical and kinetic data are known, for a set of experiments, the comparison among these corrected values with the corresponding values that can be obtained through the

experiments under the assumption of no fragmentation, can give an idea of the extent of particle breakage.

The type and degree of fragmentation affects the evolution of the curve of the overall resistance to combustion.

It must be stressed that the fragmentation is a continuous process, while the fragmentation simulations adopted herein for the analysis of the two situations under scrutiny, were composed of a limited number of discrete steps. The results with such simple approaches are, however, clear enough to assess how important is the fragmentation process during the fluidized bed batch combustion of coke.

References

[1] P.L. Waters, Factors influencing the fluidised combustion of low-grade solid and liquid fuels, Inst. Fuel Symp. Ser. N1 Fluidised Combust. 1 (1975) C6.1.
[2] B.M. Gibbs, A.B. Hedley, A pilot plant study of large coal combustion in a fluidised bed, in: Proceedings of the Seventeenth Symposium (International) on Combustion, The Combustion Institute, 1979, p. 211.
[3] R.B. Peel, F.J. Santos, Fluidised bed combustion of vegetable fuels, Inst. Energy Symp. Ser. Fluidised Combust.: Syst. Appl. 4 (1980) IIB-2-1.
[4] K.K. Pillai, The influence of coal type on devolatilization and combustion in fluidized beds, J. Inst. Energy 54 (September) (1981) 142.
[5] K.K. Pillai, Devolatilization and combustion of large coal particles in a fluidized bed, J. Inst. Energy 58 (March) (1985) 3.
[6] I.B. Ross, J.F. Davidson, The combustion of carbon particles in a fluidised bed, Trans. I. Chem. E 59 (1981) 108.
[7] C.M.C.T. Pinho, J.R.F. Guedes de Carvalho, The combustion of coke particles in a fluidised bed. Some aspects of kinetic data collection, I. Chem. E Symp. Ser. 87 (1984) 77.
[8] R. Chirone, A. Cammarota, M. D'Amore, L. Massimilla, Elutriation of attrited carbon fines in the fluidized combustion of coal, in: Proceedings of the Nineteenth Symposium (International) on Combustion, 1982, p. 1213.
[9] R.D. La Nauze, K. Jung, J. Kastl, Mass transfer to large particles in fluidised beds of smaller particles, Chem. Eng. Sci. 39 (11) (1984) 1623.
[10] J.R.F. Guedes de Carvalho, M.A.N. Coelho, Comments on mass transfer to large particles in fluidised beds of smaller particles, Chem. Eng. Sci. 41 (1) (1986) 209.
[11] O.D.S. Mota, A.M.F.R. Pinto, J.B.L.M. Campos, Fluidised-bed combustion of a charge of coke with a wide distribution of particle sizes, Chem. Eng. Sci. 49 (8) (1994) 1097.
[12] P. Salatino, L. Massimilla, A descriptive model of carbon attrition in the fluidized combustion of coal char, Chem. Eng. Sci. 40 (10) (1985) 1905.
[13] J.F. Stubington, B. Moss, On the timing of primary fragmentation during bituminous coal particle devolatilization in a fluidized bed combustor, Can. J. Chem. Eng. 71 (1995) 505.
[14] A. Williams, M. Pourkashanian, J.M. Jones, Combustion of pulverised coal and biomass, Prog. Energy Comb. Sci. 27 (2001) 587.
[15] H. Zhang, K. Cen, J. Yan, M. Ni, The fragmentation of coal particles during the coal combustion in a fluidized bed, Fuel 81 (2002) 1835.
[16] V.P. Zhukov, A.A. Ogurtsov, H. Otwinowski, D. Zbroński, Conception of a matrix model of particle attrition in fluidized bed, Powder Handling Process. 15 (6) (2003) 386.
[17] J.F. Davidson, D. Harrison, Fluidised Particles, Cambridge University Press, Cambridge, 1963.
[18] M.M. Avedesian, J.F. Davidson, Combustion of carbon particles in a fluidised bed, Trans. Inst. Chem. Eng. 51 (1973) 121.
[19] J.R.F. Guedes de Carvalho, A.M.F.R. Pinto, C.M.C.T. Pinho, Mass transfer around carbon particles burning in fluidised beds, Trans. I. Chem. E 69 (1991) 63.